



PLA as a suitable 3D printing thermoplastic for use in external beam radiotherapy

Marchant Van der Walt¹ · Tim Crabtree² · Christine Albantow¹

Received: 14 May 2019 / Accepted: 5 November 2019 / Published online: 14 November 2019
© Australasian College of Physical Scientists and Engineers in Medicine 2019

Abstract

The purpose of this paper is to investigate the tissue equivalence and radiological properties of Polylactic Acid (PLA) to determine if this material is suitable for use as a 3D printing thermoplastic for radiotherapy applications. Profiles and percentage depth-dose measurements (PDDs) were analysed for photon and electron modalities with PLA samples ($\sim 1.25 \text{ g/cm}^3$) to determine material dosimetric characteristics. Beam profiles and PDDs from treatment planning system (TPS) simulations, water tank measurements and radiochromic film measurements were compared. Tissue equivalence was determined through CT scanning several PLA samples and measuring the Hounsfield units (HUs) to determine relative electron density (RED), mass density and mass attenuation, these results were compared to several commercial tissue phantoms with varying properties. Geometric accuracy was tested by comparing digitally planned dimensions to physical and CT image measurements. Finally, resistance to radiation damage was tested by exposing PLA samples to several thousand monitor units (MUs) over several weeks and inspecting for damage. It was determined that PLA is a safe and effective thermoplastic for use as a patient specific bolus for both electron and photon treatment modalities. The material properties have been characterised and can be accurately modelled in the MONACO TPS.

Keywords 3D printing · Radiotherapy · Polylactic acid · Rapid prototyping · Monte Carlo simulation

Introduction

The advent of commercially available three-dimensional (3D) desktop printers has seen a dramatic increase in the medical applications of rapid prototyping [1]. Recent studies suggest that 3D printed, geometrically accurate and patient specific devices such as bolus are being produced for use in radiotherapy departments [2–4]. 3D printed bolus has thus far been used for quality assurance purposes and has also been employed as an alternative to traditional bolus for a fraction of the cost [4–7]. Bolus is useful for improvement of dose uniformity and to ensure the dose surface contains the PTV with 95% of the dose as recommended in ICRU report 62 [8]. It is unfortunately still the case that bolus materials such as wax may leave undesired air gaps visible

following IGRT. Using 3D printed bolus allows for a more direct match to a patient's surface as the contoured shape can be directly taken from the patient CT data set. This method of bolus creation will likely help eliminate placement irregularities between bolus and a patient's surface. As 3D printing bolus will initially constitute the primary use of 3D printing at our radiotherapy department it is necessary to characterise the material properties of this thermoplastic to ensure accurate treatment is delivered.

For rapid prototyping, most commercially available printers utilise either acrylonitrile butadiene styrene (ABS) or polylactic acid (PLA) as the thermoplastic for polymer deposition. Kairn et al. have recently investigated the use of ABS in creating tissue equivalent phantoms for radiotherapy purposes with results suggesting variable infill ABS can produce geometrically accurate and radiologically robust materials for use as lung and tissue equivalent phantoms [5]. Dancewics et al. have expanded the investigation of tissue equivalence and radiological properties to include Copperfill, Bronzefill, Photoluminescent PLA and Woodfill alongside the popular ABS and PLA. Their results indicate that 3D printed materials can accurately model various

✉ Marchant Van der Walt
marchant.vanderwalt@health.qld.gov.au

¹ Department of Medical Physics, Townsville Hospital and Health Service, Townsville 4814, Australia

² The W. P. Holman Clinic, Launceston General Hospital, Launceston 7250, Australia

tissue types for kilovoltage CT (kVCT) and megavoltage CT (MVCT) imaging modalities concluding that radiological thickness of the tested materials are comparable to standard body tissue types [9]. Mademesila et al. have reported on the radiological properties of high impact polystyrene (HIPS) for various infill values and the applications of such prints for clinical quality assurance purposes. Their results indicate that for low cost, materials with relative electron densities in clinically useful ranges can be locally manufactured [10]. Studying specifically the electron modality, Diamantopoulos et al. have investigated depth scaling factors and fluence scaling factors for PLA across multiple energies and compared to commercial TPS and standalone Monte Carlo (MC) packages with good agreement among the measured and simulated results. Their results suggest PLA can be accurately modelled through depth and fluence scaling factors [11], their study is similar to the work by Mihailescu and Borcia who studied tissue equivalence of plastic materials used in electron dosimetry using the EGSNRC Monte Carlo (MC) package [12]. Craft et al. have recently published an uncertainty analysis of popular 3D printed materials which includes ABS and PLA. Their study showed that while thermoplastics could be safely used for radiotherapy purposes, each material type should be carefully characterized for both the spread in HU and density and that poor assumptions of tissue equivalence can lead to incorrect dose distributions [13]. According to the results of Stephens et al., ultrafine particle emissions from ABS are an order of magnitude greater than for PLA [14]. There is concern that the gas phase products from thermal decomposition may release carbon monoxide and hydrogen cyanide above accepted environment levels. As such, our radiotherapy department has decided to use PLA for 3D printing. This will reduce potential risks to radiation health workers as the use of the desktop printer is set to increase.

In this study, several PLA phantoms were printed to characterize the geometric, dosimetric, tissue equivalence, and radiological properties. The aim was to assess the suitability of PLA as a 3D thermoplastic to be used clinically in a radiotherapy department and to contrast our results against published data. To investigate the clinical impact of 3D printed PLA, both photon and electron beam spectrums were utilised.

Materials and methods

PLA physical and mechanical properties

Polylactic acid is a non-corrosive thermoplastic polymer used in several plastic industries [15, 16]. So far, PLA is the most extensively studied and researched aliphatic polyester. PLA has become an industry leading biomaterial, replacing

Table 1 Ultimaker 2 + Print settings used for PLA study

Print settings Ultimaker 2 +	
Nozzle diameter	0.4 mm
Filament thickness	2.85 mm
Bed temperature	70 °C
Platform type	Glass
Nozzle temperature	190 °C
Initial layer height	0.5 mm
Layer height	0.3 mm
Line width	0.35 mm
Shells	1
Infill %	Varied
Printing pattern	Rectilinear
Print speed	50 mm/s
Initial layer speed	25 mm/s
Adhesion type	Brim
Flow % (extrusion multiplier = 1)	100

Table 2 Measured physical properties of PLA material and water [4]

Physical property	PLA	Water
Chemical formula	(C ₃ H ₄ O ₂) _n	H ₂ O
Hydrogen content (by mass)	6%	11.1%
Specific gravity	1.27	1
Solid density	1.252	–
Melt density	1.073	–
Relative electron density	1.14	1
Effective Z	4.22	3.33

many petrochemical based polymers, as such; PLA is being used for numerous applications in medicine [16]. It is one of many material types available for desktop 3D printing and provides a straightforward process when the correct settings and printing environment are established. Table 1 illustrates the print settings suitably determined for successful prints which appear to be common in the literature and among hobbyists [4]. These settings allow for prints free of warping and pooling of material due to temperature and extrusion settings. The physical and chemical properties of PLA that are of interest as a material are listed in Table 2.

Phantom design for photon and electron beam investigation

For the photon investigation, an Ultimaker2 + (Ultimaker B.V, Geldermanser, Netherlands) desktop printer was used to create five cylindrical insert phantoms measuring 28.4 mm in diameter and 70 mm in height. The top and bottom layers together with the wall thickness provided a 100% infill 1 mm shell for the cylinders visible in Fig. 1. For the

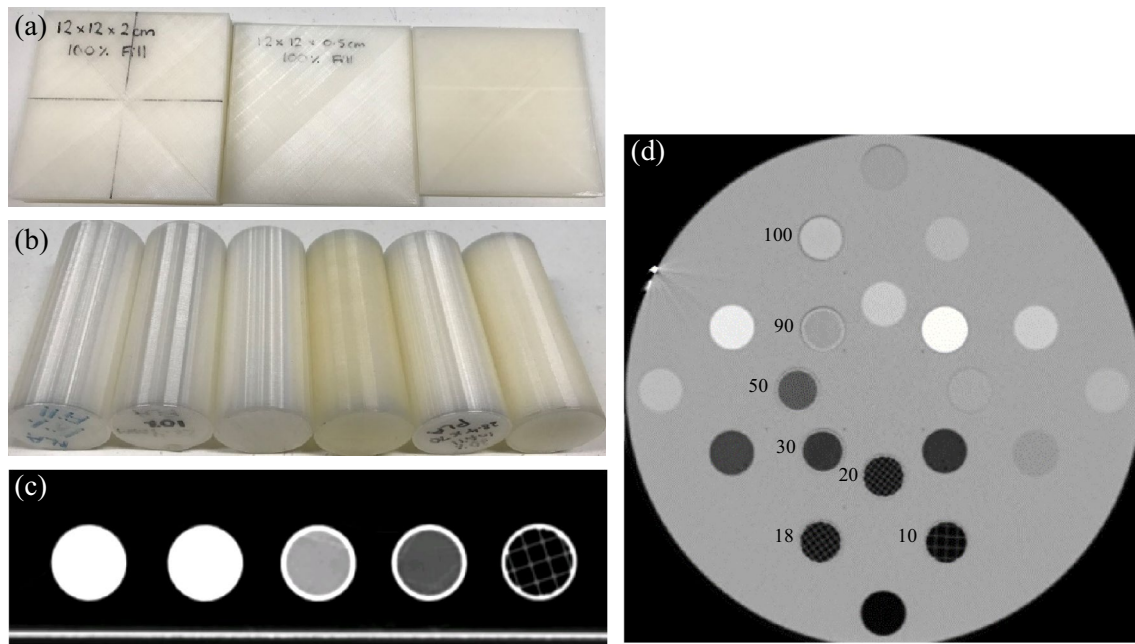


Fig. 1 **a** Various thickness 100% infill square PLA blocks used for electron dosimetry investigation. **b** Cylindrical inserts used for CT data analysis. **c** CT data set used to simulate photon beams through PLA cylinders. From left to right the cylinders are 100, 90, 50, 30 and 10%. Air gaps in low density infill printing pattern visible for 30

and 10% cylinders on right hand side. Cylinder shell becomes more apparent right to left. **d** CT data set of the GAMMEX tissue characterisation phantom with variable infill cylinders (labelled), air gaps visible for inserts below 30%

electron investigation, several 100% infill square phantoms were printed measuring $109.5 \times 109.5 \times (10, 20 \text{ and } 30)$ mm, the top and bottom layers provided a 1 mm 100% infill shell. All prints were completed using PLA ($C_3H_4O_2$)_n with a physical density of $\sim 1.25 \text{ g/cm}^3$ ($1.21\text{--}1.41 \text{ g/cm}^3$ depending on batch and impurities). The printer has a positional accuracy ≤ 12.5 microns in X and Y and ≤ 5 microns in Z with a layer resolution of 600–20 microns using a print nozzle measuring 0.4 mm; fine details in custom prints is thus possible for future prints.

The cylindrical phantoms were designed using 3D Slicer v4.10.1 [17] to fit inside a GAMMEX CT-ED phantom (GAMMEX RMI, Middleton, USA); used for CT quality control this is similar to the investigation by Dancewicz et al. [9]. This method enabled use of the same scanning and analysis protocol as our monthly QA on manufactured inserts for comparison using a known CT-ED relationship. The cylinders were printed using a rectilinear pattern and infill densities of 100, 90, 50, 30 and 10%. The electron square prints were custom designed to have sufficient coverage downstream of a 100 mm \times 100 mm Elekta Synergy electron applicator. The phantoms were custom prepared in Cura v2.1.2 (Ultimaker B.V, Geldermanser, Netherlands) from physical measurement dimensions and measured approximately $120 \times 120 \times (5, 10, 20)$ mm. All phantoms were then CT scanned on a Toshiba Aquilion dual energy

CT using a 120 kVp protocol with 3 mm slice thickness and exported to the Monaco TPS (Elekta, Crawley, UK) v5.11.01 for beam simulation analysis.

Tissue equivalence

Similar to the work of Kairn et al. and Dancewicz et al. [5, 9], this investigation studied the tissue equivalence of various infill density PLA phantoms. Firstly the 10 mm 100, 90 and 50% infill square PLA phantoms were used to determine the water equivalence (water equivalent radiological thickness as describe by Dancewicz et al. [9]) of post-print PLA via charge measurements collected downstream of a phantom resting on a 100 mm block of Solid Water (GAMMEX RMI, Middleton, USA), using a Semiflex model 31,010 ionisation chamber (PTW, Freiburg, Germany) with a constant SSD of 1000 mm to the top of the chamber holder and a $3 \times 3 \text{ cm}^2$ narrow beam geometry. An equivalent charge reading was achieved by removing the PLA blocks and placing incremental thicknesses of attenuating solid water to the top of the chamber holder. Although Dancewicz et al. used a different methodology; this factor was described as the effective relative electron density or RED_{Eff} [9]. The tissue equivalence of each of the various infill density cylindrical phantoms was analysed by CT scanning the phantoms inside the GAMMEX 465 tissue characterisation phantom

and importing them into the Monaco TPS. The HU and RED of the cylinders were measured with a sufficient region of interest (ROI) excluding the 1 mm shell for comparison to existing tissue inserts of the GAMMEX 465 tissue characterisation phantom.

Beam interaction

Photon beam interaction was measured via two methods. Firstly, percentage depth doses (PDDs) and profiles were measured by using a custom jig allowing for the suspension of the cylinders on the water surface of a PTW MP3 acrylic water tank (PTW, Freiburg, Germany), and measuring charge (nC) downstream using a PTW 31,010 Semiflex ionization chamber (PTW, Freiburg, Germany) for each of the infill density cylinders. Profiles were measured at depths of 20 mm, 50 mm and 100 mm with PDDs measured to a depth of 200 mm. Measurements were compared to PDDs and profiles simulated in the Monaco TPS from cylinder CT scans, this was done for Collapsed Cone Convolution (CCC) and MC calculation methods. Secondly, for comparison, profiles were measured using Gafchromic EBT3 radiochromic film (Ashland Advanced Materials, NJ, USA) which like the water tank measurements were performed at depths of 20, 50 and 100 mm. The gamma index as presented by Low et al. [18] was calculated for each of the photon profiles and PDDs using nominal distance to agreement (DTA) and dose criteria of 1 mm and 1% respectively.

For the electron beam interaction only 100% infill was considered and measured by using a custom jig enabling the suspension of square PLA phantoms directly on the water surface of the PTW MP3 water tank. PDDs, in-plane and cross-plane profiles were measured for 6, 8, 10 and 15 MeV beams at 50 mm depth conformed by a 100 mm × 100 mm electron applicator with standard insert. These results were compared to simulated TPS electron Monte Carlo (eMC) data using the same square phantoms. The phantoms for both the photon and electron investigations were water tight with no water draining post measurement.

Radiation damage & geometric accuracy

Phantom geometries were attained post production by physical calliper measurement and CT scan analysis for comparison to the baseline design values. Measurements were repeated post irradiation to assess any geometric deformation or induced chemical change from prolonged exposure to MV radiation. PLA bolus prints used clinically are to be discarded post treatment cycle due to being patient specific, which drastically reduces the radiation exposure to the phantoms compared to the 3D printed phantoms used for commissioning. All exposures of the PLA phantoms were carried out on an Elekta Synergy Linac over a period

spanning approximately one month. Several thousand MU's were delivered to the testing prints approximately 50 mm downstream of the mylar exit window using a leaf limits (400 mm × 400 mm) open field setup and a 6 MV photon beam.

Results

Figures 2 and 3 represent the calibration curves determined through the RED and infill % relationship for PLA. The Pearson's correlation coefficient showed an excellent linear relationship ($r^2 \geq 0.9996$) enabling an infill value to be determined for a RED of 1.000. Table 3 summarizes the comparison of PLA samples with known tissue characterisation phantom properties and with published 3D printed material properties; with column 1 listing the type of material and remaining columns listing the calculated mass density, measured mass density, relative electron density, RED_{Eff} , HU and relative linear attenuation coefficient. Table 4 lists the digital design, physical and CT data measurements for the sample geometries pre and post-radiation exposure to determine radiation induced deformity. Table 5 lists the values for the gamma analysis performed for the 6 MV photon data, a 1% dose and 1 mm DTA tolerance was set. Figure 4 illustrates the PDD comparisons between measured and simulated data for the 50, 90 and 100% infill cylinders. Figure 5 illustrates the 6 MV profile measurements that were performed at 50 mm depth for the 50, 90 and 100% infill PLA cylinders respectively. Profile comparisons were performed between MC, CCC, radiochromic film, and water tank measurements. Simulated data include MC and CCC beam data. Tables 6 and 7 list the depth of 50 and 80% dose (R_{50} , R_{80}) values for the electron beam measurements respectively, which are well within internal and international tolerances. Values were calculated from PDD data illustrated in Fig. 6 for the comparison between the linac measured and the TPS electron MC simulations. Figure 7 illustrates the comparison between the TPS and measured electron profiles, results have been highlighted for the 6 and 15 MeV beams.

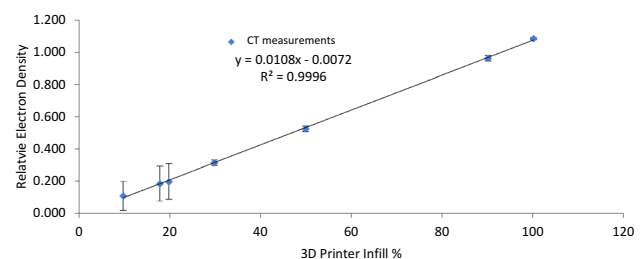


Fig. 2 Relative electron density relationship to infill % showing larger standard deviation for greater air gap values at lower infill %

Fig. 3 CT-ED relationship determined for the Toshiba Aquilion CT unit at the TCC. Final low relationship used to determine the RED for several PLA prints

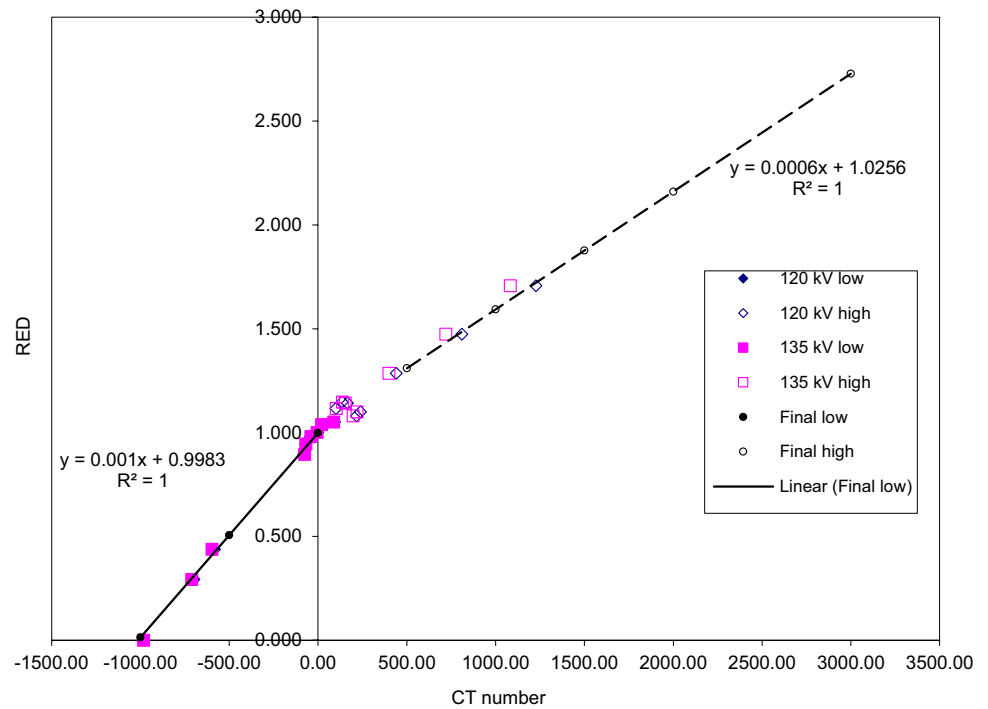


Table 3 CT data for PLA cylinders contrasted against common CT phantoms and the results of Dancewicz et al. [9]

Phantom	ρ_{calc} (g/cm ³)	ρ_{meas} (g/cm ³)	RED	REDEff	HU	μ (rel)
Cylinder—100% PLA	1.170 ± 0.007	1.173	1.085 ± 0.007	1.058 ± 0.01	138 ± 12	1.128 ± 0.007
Cylinder—90% PLA	0.983 ± 0.017	1.009	0.963 ± 0.017	0.956 ± 0.01	-39 ± 17	0.965 ± 0.017
Cylinder—50% PLA	0.545 ± 0.017	0.564	0.527 ± 0.017	0.555 ± 0.01	-482 ± 17	0.531 ± 0.017
Cylinder—30% PLA	0.318 ± 0.017	0.344	0.317 ± 0.017	0.382 ± 0.01	-693 ± 17	0.320 ± 0.017
Cylinder—10% PLA	0.086 ± 0.090	0.111	0.113 ± 0.090	-	-898 ± 90	0.124 ± 0.090
Dancewicz et al. 90% PLA	-	1.04 ± 0.03	1.01 ± 0.03	-	8 ± 4	-
Dancewicz et al. 50% PLA	-	0.550 ± 0.05	0.540 ± 0.05	-	-	-
CT-ED Brain Model #481	-	1.049	1.009 ± 0.009	-	8 ± 10	-
CT-ED Liver	-	1.039	1.055 ± 0.005	-	89 ± 8	1.089 ± 0.005
CT-ED Cortical Bone	-	1.819	1.712 ± 0.012	-	1207 ± 20	2.207 ± 0.012
CT-ED Adipose	-	0.920	0.922 ± 0.01	-	-100 ± 20	0.900 ± 0.01
CT-ED Lung 300	-	0.300	0.312 ± 0.026	-	-690 ± 80	0.310 ± 0.026
CT-ED Lung 450	-	0.450	0.427 ± 0.026	-	-560 ± 80	0.440 ± 0.026
CT-ED Breast Model	-	0.980	0.957 ± 0.015	-	-50 ± 15	0.950 ± 0.015
RT Wax Bolus	-	0.864	0.871 ± 0.003	-	-131 ± 3	0.869 ± 0.003
CT-ED Solid Water	-	1.046	1.016 ± 0.005	-	31 ± 5	1.031 ± 0.005
Water	-	1.000	1.000	-	-1.9 ± 29.6	1.000

Discussion

Tissue equivalence

Water equivalent radiological depth or RED_{Eff} was measured within the build-up region for a 6 MV photon beam as this is the environment where the PLA material is likely

to be used as a bolus agent. We feel this is an adequate measurement position to determine RED_{Eff} as it is in this region where agreement with RED measured in the TPS will be most valued. There is excellent agreement for the 100, 90, 50 and 30% infill prints when comparing to the CT measured RED. There are some deviations between RED and RED_{Eff}, while our discrepancies are not as high as reported by Dancewicz et al. for the 50 and 30% infills,

Table 4 Pre- and post-photon beam interaction geometric measurements

PLA phantoms	Radius (mm)	Length (mm)	Meas. method	Post radiation diff
100% PLA cylinder	13.7	70	Cura (design)	–
100% PLA cylinder	13.7	70	Callipers	0%
100% PLA cylinder	13.7 ± 1.0	70 ± 1.0	CT	0%
90% PLA cylinder	13.7	70	Cura (design)	–
90% PLA cylinder	13.7	70	Callipers	0%
90% PLA cylinder	13.7 ± 1.0	70 ± 1.0	CT	0%
50% PLA cylinder	13.7	70	Cura (design)	–
50% PLA cylinder	13.7	70	Callipers	0%
50% PLA cylinder	13.7 ± 1.0	70 ± 1.0	CT	0%
30% PLA cylinder	13.7	70	Cura (design)	–
30% PLA cylinder	13.7	70	Callipers	0%
30% PLA cylinder	13.7 ± 1.0	70 ± 1.0	CT	0%
10% PLA cylinder	13.7	70	Cura (design)	–
10% PLA cylinder	13.7	70	Callipers	0%
10% PLA cylinder	13.7 ± 1.0	70 ± 1.0	CT	0%

No physical variation measured

Table 5 RMS Gamma Index results for 6 MV MC vs Measured photon data with a gamma index criterion of 1% dose and 1 mm DTA

Infill	100%	90%	50%
6 MV PDDs	0.51	0.79	0.49
6 MV profiles	0.82	0.85	0.45

these deviations are likely due to the mass density effects also discussed by Danciewicz et al. [9]. From the measured data in Table 3 it is evident that the various PLA cylinders exhibit relative electron densities and linear attenuation values consistent within the range of known commercially available tissue phantoms. However, Craft et al. have shown that measured mass densities for various thermoplastics do not match well to the calculated mass densities when using their HU to density calibration curve [13]. We have found similar results for our PLA cylinders when converting from RED to physical mass density. The data from Table 3 shows that when deviating from 100% infill, we can expect correction factors from 1.026–1.077 depending on infill density, this is consistent with the results of Craft et al. [13].

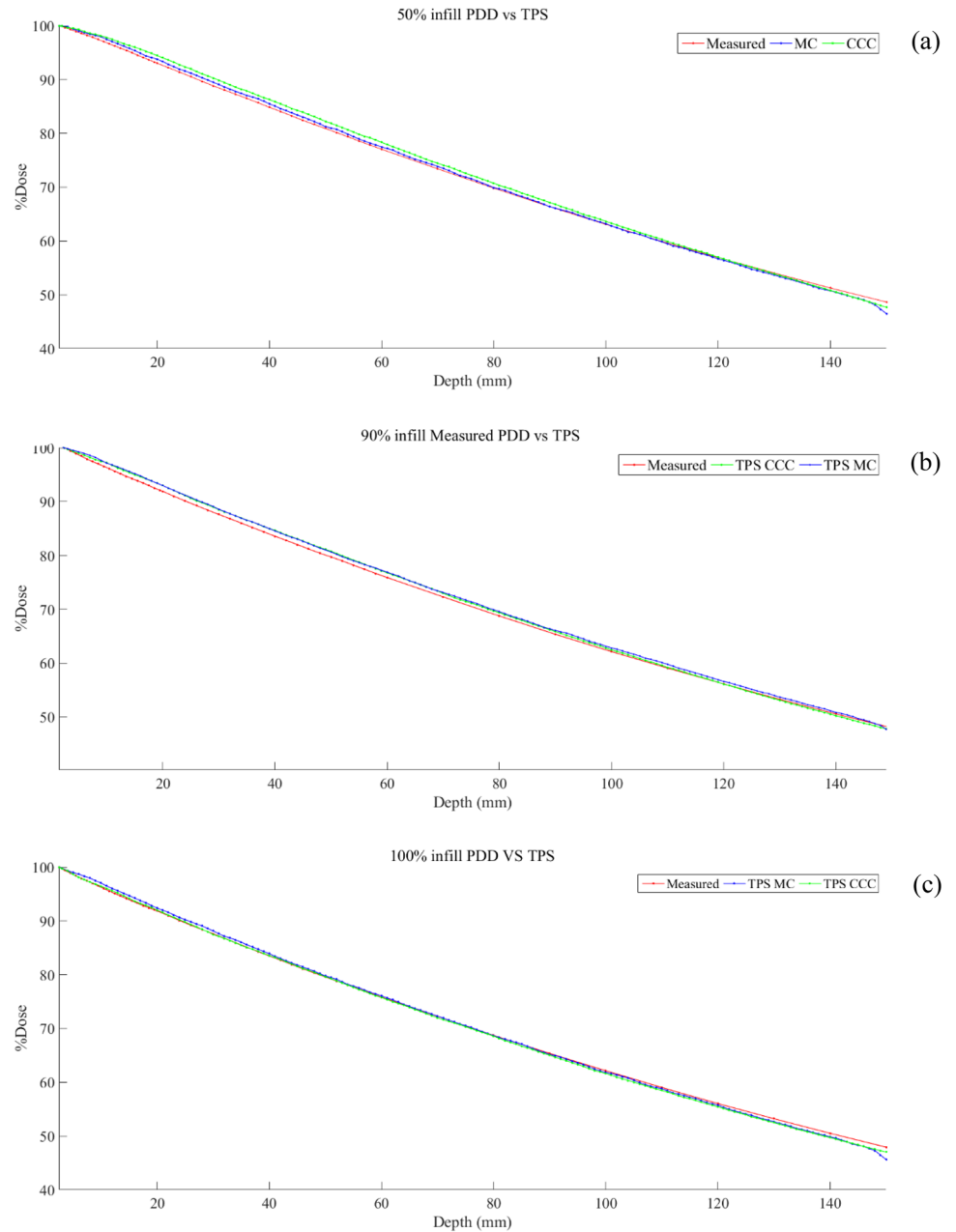
The measured properties of the 100% PLA cylinder phantom resemble the characteristics of the liver insert which potentially makes the 100% PLA print a suitable candidate for printing approximate muscle, tumour or other soft tissues types. The results for our 90% PLA phantom are within 5% to that measured by Danciewicz et al. and lie between that of adipose tissue, breast tissue and solid water [9]. This suggests printing equivalent breast tissue or adipose tissue

for dosimetric analysis is potentially viable in future. The 100% and 90% infill can be adjusted to closer approximate known bolus values such as wax used in clinical IMRT/VMAT scenarios, and 3D printed bolus has been shown to improve surface contact [19] and thereby enhance the accuracy of dose delivery.

It is currently common practice to force bolus values in our TPS to that of water, however, we have found that relative electron densities can vary by greater than 10% from that of water for some commonly used bolus types. Communication with the vendor suggests that the Monaco TPS dose calculation algorithm is sensitive to small variations in RED. Thus, determining an infill % where RED is equivalent to that of water could potentially be beneficial for patient treatment. Using the relationship derived from Fig. 2, an infill of ~93.0% should provide a print with a close approximate RED of 1.000. The results for the 30% PLA print lie between those of the two GAMMEX lung inserts (LN300, LN450) potentially making it a suitable candidate for printing anthropomorphic lung phantoms. The properties of the 50% PLA are effectively the same as that measured by Danciewicz et al. [9] with a slight variation in the uncertainty. The infill amount for the 50% print can be slightly altered to bring it closer to that of the LN450 lung insert making it another infill candidate for low - medium density lung phantoms.

Due to the grid like printing pattern (visible in Fig. 1d), results for the 10% PLA cylinder indicated a substantially large standard deviation in the density and attenuation values; large air gaps between the lattice wall structures are clearly visible on the CT scans. This is true for the 30% PLA cylinder also; however much more pronounced

Fig. 4 Measured and TPS (MC, CCC) simulated 6MV photon PDD comparisons for **a** 50% infill **b** 90% infill and **c** 100% infill



for the 10% infill, it would be preferential not to print at a lower infill than 30%, this result was also reported by Kairn et al. for the ABS material type [5]. Figure 2 illustrates the relationship we have determined for RED and infill %. We report a similar result to the investigation by Mademesila et al. who studied HIPS as a thermoplastic [10] that below a certain infill value the spread in RED due to airgaps becomes a significant source of error; this was more pronounced for HIPS compared to our PLA data.

Geometric accuracy & radiation damage

Phantom dimensions were determined such that they fit inside the Gammex tissue characterisation phantom. Dimensional measurements were performed post print production using callipers and CT scans, these measurements can be seen in Table 4. The cylinders were then subject to extensive radiation exposure, far greater than would be used in actual patient treatments. Dimensional measurements were repeated, and differences recorded

Fig. 5 Simulated (TPS MC, TPS CCC) and measured (Water tank, Film) 6MV dose profiles at 50 mm depth for **a** 50% infill and **b** 90% infill and **c** 100% infill cylinders

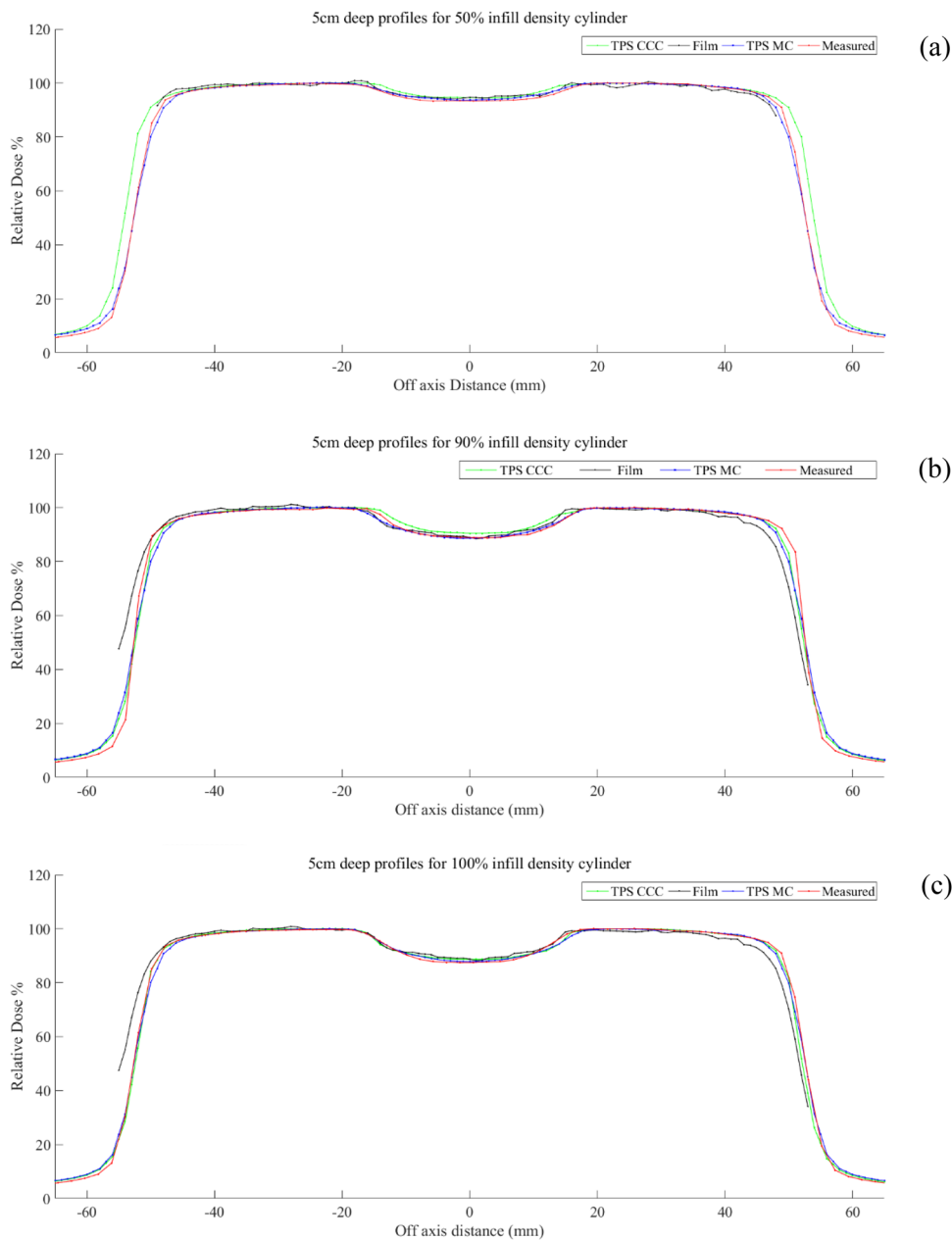


Table 6 R_{50} comparison values for TPS and linac measured using a 2 mm voxel grid size and dummy beam

Energy (MeV)	6	8	10	15
TPS R50	15.77	24.68	32.22	51.85
Linac R50	16.05	25.26	32.70	51.38

Table 7 R_{80} comparison values for TPS and linac measured using a 2 mm voxel grid size and dummy beam

Energy (MeV)	6	8	10	15
TPS R80	11.49	19.05	25.78	41.78
Linac R80	11.85	19.54	26.25	41.54

in Table 4. It is evident from measurement that despite substantial radiation exposure, PLA geometry remains unaffected with no visible radiation damage to report. Considering the MU count required to deliver a standard

IMRT head and neck is substantially lower, product failure regarding radiation damage during treatment is highly unlikely.

Fig. 6 Simulated (electron MC) and measured (water tank) PLA PDD comparisons for **a** 6 MeV **b** 8 MeV **c** 10 MeV and **d** 15 MeV beams

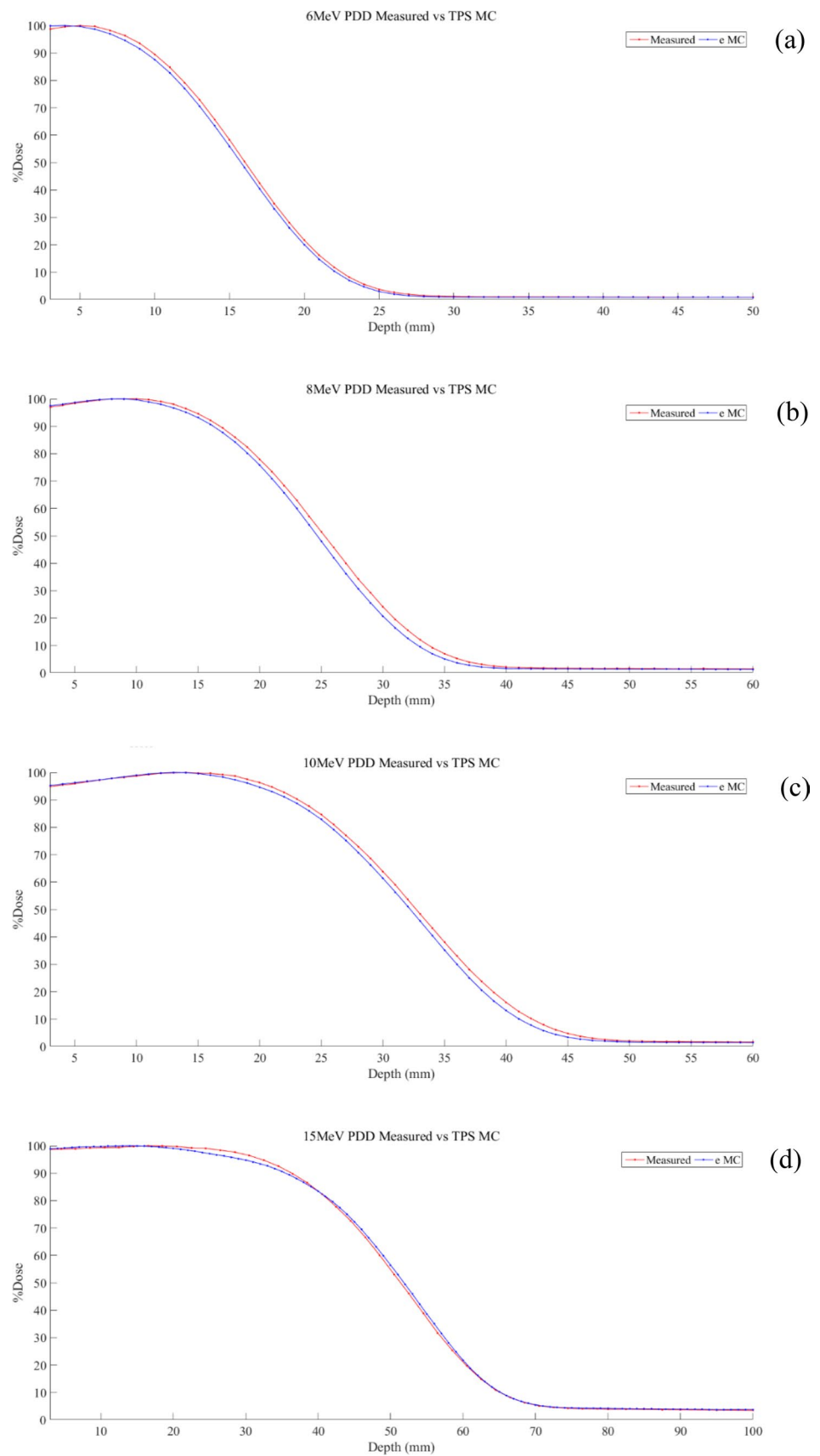
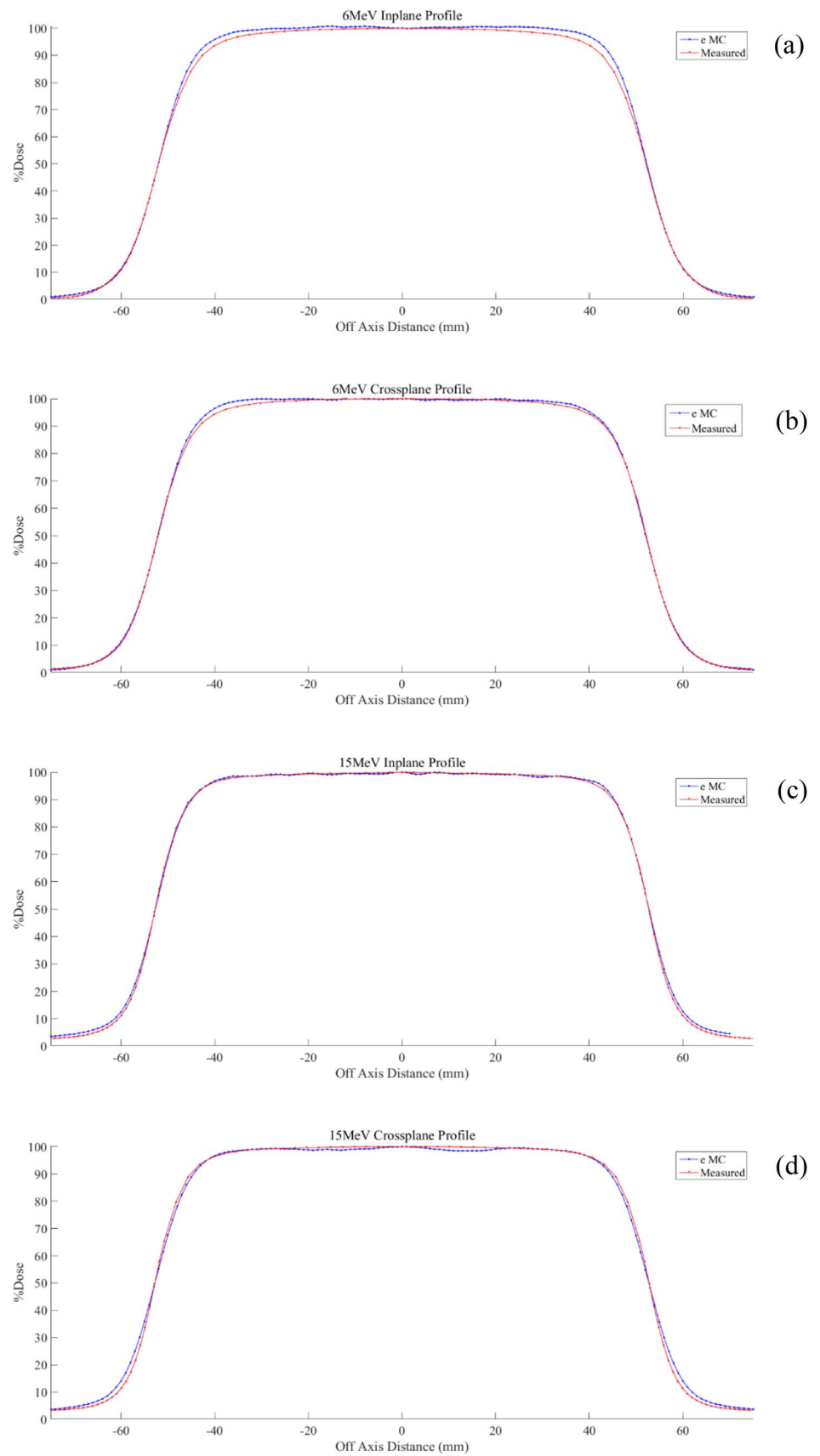


Fig. 7 Measured and simulated profiles for PLA slabs at 50 mm depth for **a** 6 MeV inplane **b** 6 MeV crossplane **c** 15 MeV inplane and **d** 15 MeV crossplane



Beam interaction

Photons

PDDs and profiles were measured for each of the percentage infill density cylinders with results highlighted for the 100, 90 and 50% cylinders and profile data taken at a depth of 50 mm.

Physical measurement within the PLA cylinder was not possible; therefore, measurement begins at the cylinder - water interface. All TPS data has been calculated with a 0.1% uncertainty per control point using the MC algorithm and the collapsed cone convolution (CCC). When simulating beams, the native CT data of each cylinder was used without forcing a homogenous RED. A gamma index criterion of 1% dose and 1 mm DTA was used for comparison calculations with results shown in Table 5. The photon profile measurements are illustrated in Fig. 5, with the data displaying excellent agreement among the various measurement methods and results are well within a tolerance of 10% as used by Kairn et al. [5]. Overall there is excellent agreement between measured and simulated data for the PLA photon beam interactions.

Electrons

Electron PDDs and profiles were measured downstream of a 120×120×10 mm square 100% infill PLA print depicted in Fig. 1a. These results were compared to the TPS beam simulations of the square PLA CT data set. Comparative doses of 50% and 80%, R_{50} and R_{80} respectively, have been recorded and are available in Tables 6 and 7. A standard voxel or grid size of 2 mm was used for the TPS simulations as this is what is currently used clinically for patient treatment plans as opposed to a 1 mm grid.

Currently, using a 2 mm voxel grid will produce an error of approximately 1 mm in the raw dose grid where dose is deposited outside of the phantom contour, which while not a significant problem for photon beams, a 1 mm shift in an electron beam is significant. TPS vendor support advised the use of a dummy beam with 0 MUs to help eliminate voxel averaging effects, resulting in greater accuracy in beam data by correctly positioning the dose grid (Elekta, Crawley, UK). From Tables 6 and 7 it is evident that the TPS beam simulations match the linac measurements within the ± 2 mm international tolerance and the ± 1 mm internal tolerance post dummy beam correction.

Conclusion

It has been demonstrated that a relatively inexpensive desktop 3D printer utilising a suitable thermoplastic can be made clinically available in a radiotherapy department.

PLA samples were tested to determine if the 3D thermoplastic could be used as a patient specific bolus. Comparative analysis has shown for varying degrees of infill % PLA the thermoplastic can be used to simulate materials in the relative electron density range 0.01–1.10. It was determined that PLA samples can be accurately modelled in the Monaco TPS. Samples of PLA were subject to beams delivering a substantial MU count and have been shown to retain physical properties. A radiotherapy department wishing to utilise 3D printing for the purpose of custom bolus creation will need to perform measurements similar to what is contained in this work. By characterising the radiological and dosimetric properties as has been done here will enable a radiotherapy department to create a patient specific bolus safely and effectively.

Compliance with ethical standards

Conflict of interest All authors declare that they have no conflict of interest.

Ethical approval This article does not contain any studies with human participants or animals performed by any of the authors.

References

- Schubert C, van Langeveldt M, Donors L (2013) Innovations in 3D printing: a 3D overview from optics to organs. *Br J Ophthalmol* 98(2):159–161
- Zou W, Fisher T, Zhang M, Kim L, Chen T, Narra V, Swann B, Singh R, Siderit R, Yin L, Teo B, Mckenna M, McDonough J, Ning Y (2015) Potential of 3D printing technologies for fabrication of electron bolus and proton compensators. *J Appl Clin Med Phys* 16(3):90–98
- Su S, Moran K, Robar J (2014) Design and production of 3D printed bolus for electron radiation therapy. *J Appl Clin Med Phys* 15(4):194–211
- Park S, Choi C, Park J, Chun M, Han J, Kim J (2016) A patient-specific polylactic acid bolus made by a 3D printer for breast cancer radiation therapy. *PLoS ONE* 11(12):e0168063
- Kairn T, Crowe S and Markwell T (2015) Use of 3D printed materials as tissue-equivalent phantoms. *IFMBE Proceedings*, pp.728–731.
- Kim S, Shin H, Kay C, Son S (2014) A customized bolus produced using a 3-dimensional printer for radiotherapy. *PLoS ONE* 9(10):e110746
- Burleson S, Baker J, Hsia A, Xu Z (2015) Use of 3D printers to create a patient-specific 3D bolus for external beam therapy. *J Appl Clin Med Phys* 16(3):166–178
- Landberg T, Chavaudra J, Dobbs J, Gerard JP, Hanks G, Horiot JC, Johansson KA, Möller T, Purdy J, Suntharalingam N, Svensson H (1999) Report 62. *J Int Comm Radiat Units Meas*. <https://doi.org/10.1093/jicru/os32.1.Report62>
- Dancewics OL, Sylvander SR, Markwell TS, Crowe SB, Trapp JV (2017) Radiological properties of 3D printed materials in kilovoltage and megavoltage photon beams. *Phys Med* 38:111–118
- Madamesila J, McGeachy P, Barajas JE, Khan R (2015). Characterizing 3D printing in the fabrication of variable

- density phantoms for quality assurance of radiotherapy. *Phys Med* 32:242–247
11. Diamontopolous S, Kantemiris L, Patatoukas G, Dilvoi M, Efstathopoulos E, Kouloulis V, Platoni K (2018) Theoretical and experimental determination of scaling factors in electron dosimetry for 3D printed polylactic acid. *Med Phys* 45(4):1708–1714
 12. Mihailescu D, C. B. (2006) Water equivalency of some plastic materials used in electron dosimetry: a Monte Carlo investigation. *Rom Rep Phys* 58(4):415–425
 13. Craft DF, Peter Balter SFK, Salehpour M (2018) Material matters: Analysis of density uncertainty in 3D printing and its consequences for radiation oncology. *Med Phys* 45(4):1614–1621
 14. Stephens B, Azimi P, El Orch Z, Ramos T (2013) Ultrafine particle emissions from desktop 3D printers. *Atmos Environ* 79:334–339
 15. Castro-Aguirre E, Iñiguez-Franco F, Samsudin H, Fang X, Auras R (2016) Poly (lactic acid)—mass production, processing, industrial applications, and end of life. *Adv Drug Deliv Rev.* <https://doi.org/10.1016/j.addr.2016.03.010>
 16. Farah S et al (2016) Physical and mechanical properties of pla, and their functions in widespread applications—a comprehensive review. *Adv Drug Deliv Rev* 107:367–392
 17. Pieper S, Lorensen B, Schroeder W, Kikinis R (2006) The NAMIKit: ITK, VTK, pipelines, grids and 3d slicer as an open platform for the medical image computing community. In: Proceedings of the 3rd IEEE international symposium on biomedical imaging: from nano to macro, vol. 1, pp. 698–701
 18. Low DA, Harms WB, Mutic S, Purdy JA (1998) A technique for the quantitative evaluation of dose distributions. *Med Phys* 25(5):656–661. <https://doi.org/10.1118/1.598248>
 19. Albantow C, Brown A, Hargraves C, Halsall C (2019) unpublished results (pending). *J Med Radiat Sci*

Publisher's Note Springer Nature remains neutral with regard to jurisdictional claims in published maps and institutional affiliations.